

# Shannon Entropy in Stochastic Analysis of Some Mems

Marcin Kamiński <sup>1,\*</sup> and Alberto Corigliano <sup>2</sup><sup>1</sup> Department of Structural Mechanics, Łódź University of Technology, 90-924 Łódź, Poland<sup>2</sup> Department of Civil and Environmental Engineering, Politecnico di Milano, 20133 Milano, Italy; alberto.corigliano@polimi.it

\* Correspondence: marcin.kaminski@p.lodz.pl

**Abstract:** This work is focused on the numerical determination of Shannon probabilistic entropy for MEMS devices exhibiting some uncertainty in their structural response. This entropy is a universal measure of statistical or stochastic disorder in static deformation or dynamic vibrations of engineering systems and is available for both continuous and discrete distributions functions of structural parameters. An interval algorithm using Monte Carlo simulation and polynomial structural response recovery has been implemented to demonstrate an uncertainty propagation of the forced vibrations in some small MEMS devices. A computational example includes stochastic nonlinear vibrations described by the Duffing equation calibrated for some micro-resonators, whose damping is adopted as a Gaussian, uniformly and triangularly distributed input uncertainty source.

**Keywords:** Shannon entropy; MEMS vibrations; Duffing equation; random damping

## 1. Introduction

It is well known that the probabilistic entropy of the given random variable or process represents an averaged level of uncertainty in its numerical or experimental realizations. It is also a mathematical extension of its thermodynamic origin, invented by Boltzmann, and now it may serve as a universal measure of disorder in the given engineering system. The first method of its calculation was proposed by Claude Shannon [1,2], although the term “entropy” was introduced by Johann von Neumann; this has been used multiple times to analyse disorder in various engineering systems [3]. The original definition by Shannon includes a summation of probabilities of various admissible states of the given experiment multiplied with their logarithms; such an entropy was determined from the very beginning using various estimation methods [4]. Various further extensions and modifications have been worked out independently and presented by Renyi [5,6], Tsallis [7–10], and Kolmogorov and Sinai [11,12]. They are available now for both discrete and continuous probability distributions of the stochastic response for a given engineering system, and are also applicable in some non-engineering studies [13].

Despite the calculation method, maximum entropy is equivalent to minimum knowledge about some phenomenon and vice versa. The majority of research related to probabilistic engineering mechanics recalls most frequently the maximum entropy principle [14,15], which states that the probability distribution giving the best representation of the current knowledge state about a given engineering system is the one having the largest probabilistic entropy.

The main numerical difficulty in probabilistic entropy calculation is the necessity of the final probability density function availability. This makes many of the stochastic computer techniques like Bayesian methods [16], Karhunen-Loeve, polynomial chaos, or stochastic perturbation technique [17] simply inapplicable; this is the reason why the traditional Monte Carlo simulation scheme [18,19] may be preferred in this context. Some studies in the area of applications of probabilistic structural dynamics have been documented in the literature [20]. An interesting alternative could be the determination of probabilistic

**Citation:** Kamiński, M.; Corigliano, A. Shannon Entropy in Stochastic Analysis of Some Mems. *Energies* **2022**, *15*, 5483. <https://doi.org/10.3390/en15155483>

Academic Editor: Mateus Mendes

Received: 24 June 2022

Accepted: 26 July 2022

Published: 28 July 2022

**Publisher's Note:** MDPI stays neutral with regard to jurisdictional claims in published maps and institutional affiliations.



**Copyright:** © 2022 by the authors. Licensee MDPI, Basel, Switzerland. This article is an open access article distributed under the terms and conditions of the Creative Commons Attribution (CC BY) license (<https://creativecommons.org/licenses/by/4.0/>).

distance (divergence) in between two probability densities, which can represent the general input signal and the output response. It can be useful in civil engineering to model limit functions, being an inherent part of reliability assessment. Such a probabilistic distance may link extreme structural effort of the given nature with its corresponding capacity (in the context of deformations and/or stresses), so it could be an alternative measure of the structural safety or may be employed for sensitivity in engineering design [21]. A huge variety of relative entropy models is available now in the literature: it is necessary to recall the Kullback–Leibler approach [22] (exhibiting a well-known lack of symmetry), Jensen–Shannon, Hellinger [23], Chernoff [24], Mahalanobis [25], or Bhattacharyya [26] probabilistic differences.

The purpose of this study is the determination of probabilistic entropy fluctuations in some micro-resonator-forced vibration problems with uncertainty described by the Duffing equation; its understanding seems to be necessary for further, more general, numerical analyses of the disorder and uncertainty propagation in nonlinear vibrations of various MEMS devices [27–29]. Let us note that entropy propagation in stochastic structural dynamics has been studied before for some elastic beams with cross-sectional uncertainty [30]. The need for randomness analysis in the case of these devices is motivated by a lot of different reasons: (i) material and geometrical imperfections, (ii) environmental actions, measurements, and vibrations (as well as their sources), (iii) statistical scattering in the shape, response and material characteristics of their structural components, (iv) coupling in-between different physical fields, phenomena and properties (thermo-electro-magneto-mechanical) and their time delay in various exploitation conditions [31]. The damping coefficient of these micro-devices is chosen as the input uncertainty source because this parameter decisively affects its dynamic response, and its probability distribution is modelled using alternatively uniform, triangular as well as Gaussian distributions; all these distributions are based on the same upper and lower bounds for the uncertainty interval. The deterministic vibrations spectrum is obtained numerically using the Runge–Kutta–Fehlberg algorithm [32] implemented in the computer algebra system MAPLE, and this is the basis for the polynomial Least Squares Method [33] approximation of the micro-resonator displacements concerning the damping coefficient. Further parts programmed in the same system include Monte Carlo sampling (MCS) of the damping parameter and the same sampling of the dynamic response and final Shannon entropy calculation using a formula adjacent to the interval representation of the statistical data. Due to the highly nonlinear character of the physical phenomenon and of the corresponding dynamic equilibrium equation, numerical simulation is the only uncertainty analysis method; analytical formulas derived and widely used for linear stochastic systems cannot be simply used in this case. The approach proposed in this work may be used for more advanced MEMS analyses using commercial Finite Element Method codes like COMSOL or ABAQUS, for computer simulation of inelastic deformation in solids, for disorder propagation analysis in various computational fluid mechanics problems.

## 2. Governing Equations of the Problem

**Problem 1.** Determine Shannon entropy  $H(y(c;t))$  for a dynamical system having a single degree of freedom and governed by the following differential equation:

$$m\ddot{y}(t) + c\dot{y}(t) + k_1y(t) + k_2y^2(t) + k_3y^3(t) = F \sin(\omega t) \quad (1)$$

where  $m$  denotes the mass of the vibrating structure,  $c$  stands, obviously, for the damping coefficient, discrete values  $k_1$ ,  $k_2$  and  $k_3$  are first, second and third-order stiffness coefficients related to various physical fields and sources,  $F$  and  $\omega$  are the amplitude and frequency of the modulation signal. External forcing has been chosen as perfectly periodic at the initial stage to verify how stationary signals affect the structural response of the MEMS. It also enables for some verification of the output signals and is frequently chosen in various theoretical and numerical studies. Initial

equation of motion is solved with traditional initial conditions equivalent to static equilibrium in the undeformed configuration:

$$y(t=0) = 0, \quad \dot{y}(t=0) = 0, \quad (2)$$

Shannon entropy is to be determined from its classical definition at any discrete-time moment  $\tau$ . It yields [3,34]:

$$H(y(c, \tau)) = -\sum_{i=1}^n p_i(y(c, \tau)) \log(p_i(y(c, \tau))), \quad (3)$$

where  $n$  denotes the total number of subintervals enabling discretization of the entire probability domain of the given structural response. Let us note that this formula could be generalized towards the continuous PDFs as

$$\hat{H}(y(c, \tau)) = -\int_{-\infty}^{+\infty} p_y(x) \log(p_y(x)) dx. \quad (4)$$

This formula would be applicable if only any reliable numerical method of determination of the density  $p_y(x)$  would be available. The majority of such an approach would be insensitivity to the output PDF partition during post-processing of the Monte Carlo simulation results. Interval analysis for estimation of the Shannon entropy [35,36] is further employed, so that: let us consider a continuous random variable  $b$  with its probability density function  $g_b(x)$  discretized by a set of subintervals of constant length  $\delta$ . The mean value theorem leads to the following representation of  $p_b(x)$  in each  $i$ th subinterval:

$$p_b(x_i) = \frac{1}{\delta} \int_{i\delta}^{(i+1)\delta} p_b(x) dx. \quad (5)$$

Let us introduce further the quantized random variable  $\hat{x}$  defined as

$$\hat{x} \equiv x_i \text{ for } i\delta \leq \hat{x} \leq (i+1)\delta, \quad (6)$$

with probability equal to

$$p_i = \int_{i\delta}^{(i+1)\delta} p_b(x) dx = \delta p_b(x_i). \quad (7)$$

According to the Shannon definition, probabilistic entropy corresponding to a partition of  $p_b(x)$  into  $n$  equal subsets equals [37,38]

$$\begin{aligned} H(\hat{x}) &= -\sum_{i=1}^n p_i \log(p_i) = -\sum_{i=1}^n \delta p_b(x_i) \log(\delta p_b(x_i)) = \\ &= -\sum_{i=1}^n \delta p_b(x_i) \log(p_b(x_i)) - \log(\delta). \end{aligned} \quad (8)$$

Finally, calculation of probabilistic moments of the structural response at any discrete-time moment  $\tau$  undergoes, using classical statistical estimators (as in [39]),

$$E[y(c, \tau)] = \frac{1}{M} \sum_{j=1}^M y_j(c, \tau), \quad (9)$$

$$Var(y(c, \tau)) = \frac{1}{M-1} \sum_{j=1}^M \{y_j(c, \tau) - E[y_j(c, \tau)]\}^2.$$

$M$  denotes in these relations the total number of random trials, while the coefficient of variation of the structural response is obtained by a ratio of standard deviation to the corresponding expectation. Further determination of probabilistic entropy for the given

MEMS device proceeds directly thanks to the determination and partition of the probability distribution function of its structural response. This in turn proceeds via the iterative solution of the following equation:

$$m\ddot{y}_{(j)}(t) + c_{(j)}\dot{y}_{(j)}(t) + k_1y_{(j)}(t) + k_2y_{(j)}^2(t) + k_3y_{(j)}^3(t) = F \sin(\omega t), \quad (10)$$

Since the damping coefficient is taken as the Gaussian input variable with expectation and standard deviation equal to  $E[c]$  and  $\sigma(c)$ , respectively, its discrete realizations are obtained via an equidistant partition of the interval  $[E[c] - 3\sigma(c), E[c] + 3\sigma(c)]$ . These discrete solutions substituted to the Least Squares Method fitting procedure enable one to determine the structural response as a polynomial of its damping, and the order of this polynomial is optimized using minimization of the fitting variance and RMS error as well as maximization of the correlation factor of the approximating polynomial to the fitting dataset. Having determined the response polynomial, one may apply the classical MCS strategy to make a histogram of this response, whose further processing results in Shannon entropy value. Such an algorithm enables the application of non-Gaussian parameters or even a couple of various uncertainty sources at the same time.

### 3. Mems Device Description

The so-called L-shaped micro-resonator is the engineering device under consideration here. It consists of two parallel electrodes (the driving one and the sensing one; see Figure 1). External acceleration includes in this resonator some longitudinal force and it is modelled as a slender beam having a constant cross-section, inertia moment, and Young's modulus. It is axially constrained at both ends and it oscillates in bending mode due to a certain electrostatic actuation. Some relaxation at one end of such a micro-resonator is modelled by introducing an equivalent axial spring. It is well known that L-shaped micro-resonators exhibit a coupled non-linear response, which consists of electrostatic non-linearity resulting from the parallel plates actuation as well as mechanical non-linearity in the axial stretching. The equation of motion of such a resonant beam including both effects may be directly derived from the Hamilton principle [40] and it is relevant to the equivalent single degree of freedom (d.o.f.) dynamic model. Needless to say, such a micro-device is very sensitive to the operation temperature range [40], but this effect has been postponed here due to the brevity of presentation and discussion.

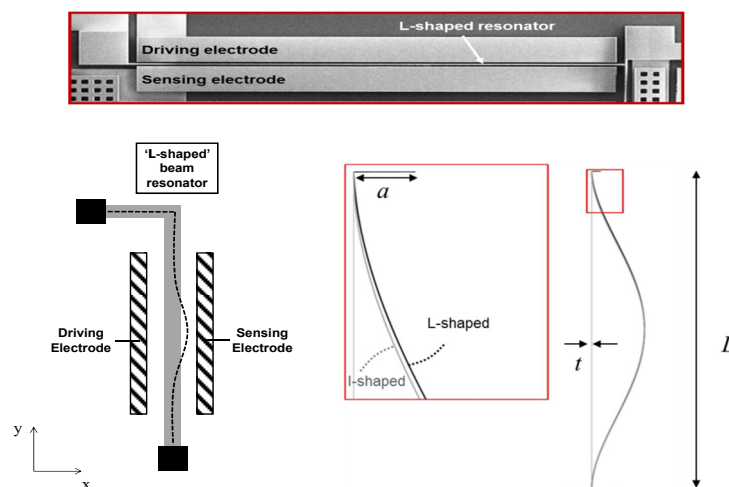


Figure 1. L-shaped micro-resonator.

Numerical analysis reported here has been completed with experimental input data adopted after [41]. Mechanical and electrical contributions  $k_m$  and  $k_e$  to the overall stiffness

of the micro-resonator are represented by the following stiffness coefficients  $k_i$ ,  $i = 1, 2, 3$ , which in turn are taken as

$$k_1 = (k_{m1} - k_{e1}) = (0.829 - 0.068) = 0.761 \text{ N/m},$$

$$k_2 = 0 \text{ N/m}^2, \quad (11)$$

$$k_3 = (k_{m3L} - k_{e3}) = (1.45 \times 10^{11} - 2.2 \times 10^{10}) = 12.3 \times 10^{10} \text{ N/m}^3.$$

The second order stiffness  $k_2$  simply vanishes for the perfect micro-resonators, where the gaps in between the resonator and driving, as well as sensing electrode are equal to each other. In this specific case, Equation (10) becomes the Duffing equation, whose further numerical solution enables stochastic response analysis. Some other physical phenomena appearing in the micro-resonators together with their mathematical consequences have been reported in detail in [40]. The effective mass of the micro-resonator was calculated in [41] from its length  $L = 400 \mu\text{m}$ , width  $t = 1.2 \mu\text{m}$ , out of the plane thickness  $w = 15 \mu\text{m}$ , the silicon mass density  $\rho = 2330 \frac{\text{kg}}{\text{m}^3}$ . The value  $m = 0.3965 \times M = 6.65 \times 10^{-12} \text{ kg}$  is obtained, using the formula that gives the equivalent mass  $m$  as a fraction of the total beam mass  $M = 16.78 \times 10^{-12} \text{ kg}$ . The mean value of the damping coefficient has been proposed using the formula  $c = \frac{1}{Q} \sqrt{km} \left[ \frac{\text{Nsec}}{\text{m}} \right]$ , where  $k$  includes all the stiffnesses introduced in Equation (1); the expected value of damping parameter  $c$  has been taken as equal to  $E [c] = [0.00394] \times 10^{-6} [\text{Nsec/m}]$  and the coefficient of variation of this physical parameter is taken further from the interval  $\alpha(c) \in [0.00, 0.20]$ . The harmonic external force representing electrostatic actuation is introduced as

$$F \sin(\omega t) = \eta v_a(t), \quad (12)$$

where

$$\eta = \alpha V_p \frac{\varepsilon_0 w L}{d^2}, \quad \alpha = 0.523, \quad V_p = 2 \div 9 [V], \quad \varepsilon_0 = 8.8541878176 \times 10^{-12} [F/m].$$

$$w = 15 \mu\text{m}, \quad L = 400 \mu\text{m}, \quad d = 2.1 \mu\text{m}, \quad v_a(t) = v_a \sin(\omega t), \quad v_a = 5 \times 10^{-3} \div 1 \times 10^{-1} [V] \quad (13)$$

In the above relations,  $\alpha$  denotes the coefficient related to the mechanical behavior of the resonator,  $V_p$  is the bias voltage,  $\varepsilon_0$  is the absolute vacuum permittivity constant,  $d$  means the gap between the oscillating beam and the electrode,  $v_a(t)$  is the actuation voltage, usually modulated at the mechanical frequency of the oscillating beam  $\omega$ . Finally, the external force has the following multiplier:  $F = 56.7 \times 10^{-10} [N]$ , while a frequency  $\omega$  has been adopted as  $10^3$ .

#### 4. Numerical Simulation and Discussion

The entire numerical simulation has been programmed and performed in the computer algebra system MAPLE 2019.2. This computational environment has been preselected because it offers a Runge–Kutta–Fehlberg numerical solution of the Duffing equation, the Least Squares Method polynomial approximations for the given discrete datasets, and also random number generators, statistical estimation of the resulting probabilistic characteristics, together with histogram creation. Some additional procedures enabling statistical optimization of approximation order, Shannon entropy estimation have been additionally implemented into a single MAPLE script. The computer system MAPLE offers also interoperability with other computer simulation systems (both academic and commercial), building and usage of the user's own Windows applications, as well as macro-procedures supervising cyclic usage of other mathematical and engineering software.

It is of paramount importance when the Monte Carlo simulation is to be carried out. It should be mentioned that neither the chosen computer system nor other commercial mathematical packages directly enable computations of probabilistic entropy in the context of differential equations solution.

A flowchart of numerical analysis programmed in the system MAPLE is schematically shown in Figure 2 below. The following notation has been adopted: (i) M means the total number of random samples in the Monte Carlo scheme, (ii) N denotes the number of discrete time moments in dynamic analysis, while (iii) P corresponds to the order of polynomial approximation, whose optimal choice is P'.

One of the most important parts in this methodology is numerical recovery of the polynomial response functions and statistical optimization of its order. They are carried out both for several input discrete damping coefficients and the corresponding structural outputs. The main goal is to find the polynomial, whose order guarantees that the polynomial is the closest to the datasets linking the damping and structural response. Such a procedure is completed at each discrete time moment for the given domain of structural vibrations. Various order fitting polynomials are numerically determined using the Least Squares Method approach (consecutively from 2 to 9) and then, the variance as well as the correlation factor are computed for all these orders. Optimal polynomial minimizes the variance (also the mean square error) and maximizes the correlation factor at the same time. It can be concluded from the results contained in Table 1 that the 4th order polynomial basis has been found as the most efficient. It is confirmed with the results shown in this table that optimal 4th order approximation minimizes the squares sum in the LSM procedure, while the differences in this parameter obtained for various orders may have a few orders of magnitude.

**Table 1.** Statistical optimization results for the polynomial response order.

Polynomial Order	Correlation	RMS Error	Squares Sum	Fitting Variance
2	0.944648	$6.50235 \times 10^{-12}$	$4.65126 \times 10^{-22}$	$4.65228 \times 10^{-23}$
3	0.999390	$7.22270 \times 10^{-13}$	$5.76870 \times 10^{-24}$	$5.86760 \times 10^{-25}$
4	0.999571	$6.09214 \times 10^{-13}$	$4.11380 \times 10^{-24}$	$2.90649 \times 10^{-24}$
5	-0.594698	$7.08217 \times 10^{-10}$	$5.51726 \times 10^{-18}$	$2.45674 \times 10^{-19}$
6	-0.924625	$8.02584 \times 10^{-9}$	$7.08554 \times 10^{-16}$	$4.98402 \times 10^{-16}$
7	0.936636	$8.11866 \times 10^{-7}$	$7.25038 \times 10^{-12}$	$3.53456 \times 10^{-12}$
8	-0.942430	$8.61679 \times 10^{-5}$	$8.16740 \times 10^{-8}$	$1.25495 \times 10^{-6}$
9	-0.937340	$6.38454 \times 10^{-4}$	$4.48386 \times 10^{-6}$	$6.55977 \times 10^{-7}$

Having an optimal polynomial basis for the structural response, we studied the uncertain behavior of the micro-resonator in terms of its first two probabilistic moments computed for the input coefficient of variation of damping equal to  $\alpha(c) = 0.10$ . Expected values and coefficients of variations have been presented in the left and the right graph of Figure 3 and they are included here for a comparison with further Shannon entropies. It is seen that initial expectations show some periodicity, but the most important conclusion is that the resulting coefficient of variation exhibits an enormously large value at a certain discrete time of the vibration process. The value larger than 1.0 was never observed in classical solid mechanics with uncertainty and follows the coupled electro-mechanical character of this phenomenon. It may be of special importance while analyzing the reliability of such a microdevice, where traditionally second order moments play a decisive role.

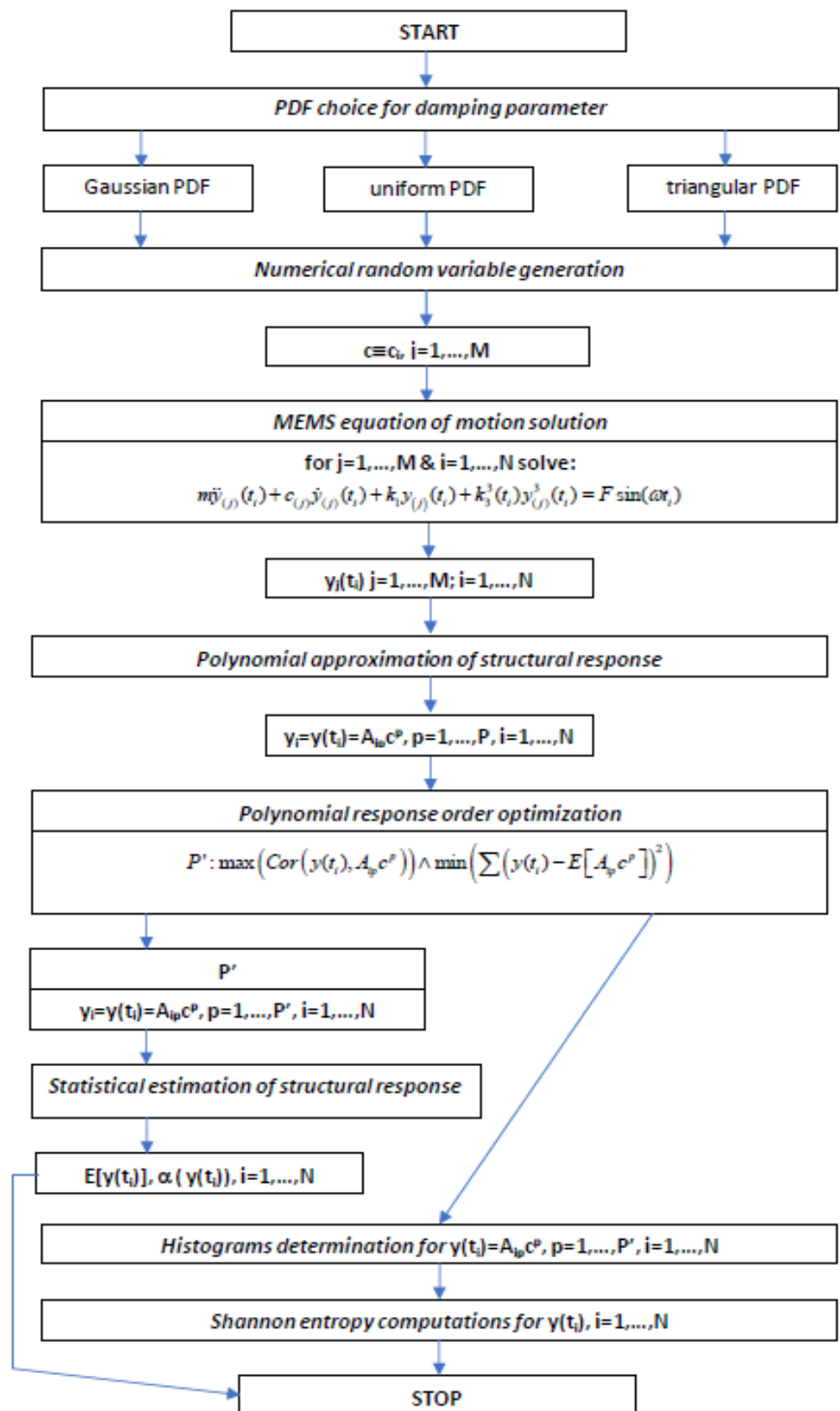
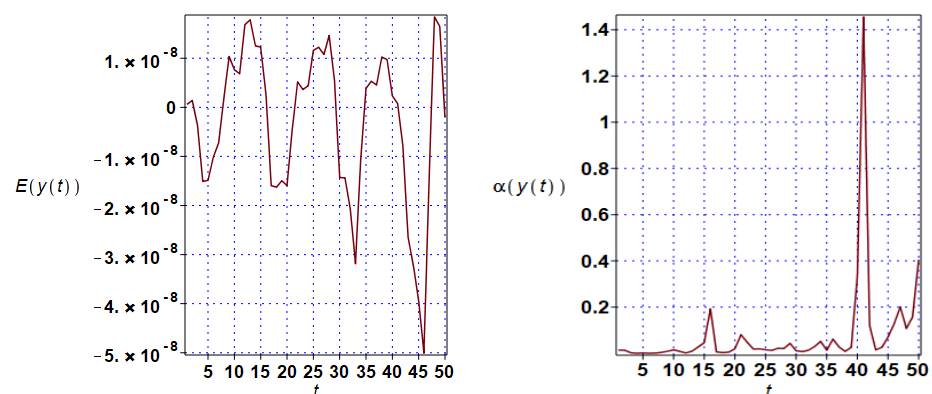


Figure 2. Flowchart of probabilistic entropy numerical simulation.

After determination of the first two moments of the structural response, it is necessary to make an initial numerical study concerning the numerical convergence of Shannon entropy (and its possible sensitivity) while increasing the partitioning density of the structural response histogram. A Gaussian random variable has been preselected for this study, and it has an expected value equal to 10, and also a few different standard deviations taken in turn as  $\sigma = [0.05, 0.10, 0.15, 0.20, 0.25, 0.30]$ . The results corresponding to the increasing number of subintervals  $n$  have been contrasted in Figure 4. It is seen that the entropy under consideration is less sensitive to this partitioning for smaller standard deviations of the given uncertainty source (especially when  $\sigma = 0.05$  here). Huge statistical dispersion (close to  $\sigma = 0.20$  and higher) needs may cause some numerical discrepancies for a smaller  $n$  close to 10 and demands each time determination of the stability region starting usually from  $n = 25$ .



**Figure 3.** The expected values of the MEMS device vibration (left) and its coefficient of variation (right).

A determination of the satisfactory partition of both input and output uncertainty guarantees efficient estimation of probabilistic entropy, which can be evaluated when the coefficient of variation reaches its extreme value. Shannon entropy is expected to be more efficient in uncertainty evaluation while periodic or quasi-periodic vibrations are analyzed, because of the huge increase of the coefficient of variation, especially when the expected value tends to 0 (cf. Figure 3, right diagram). Application of this technique to multi degrees of freedom models for MEMS is possible by replacing Equation (10) with its matrix counterpart and by determination of the optimal polynomial responses in a local manner—for each degree of freedom separately.

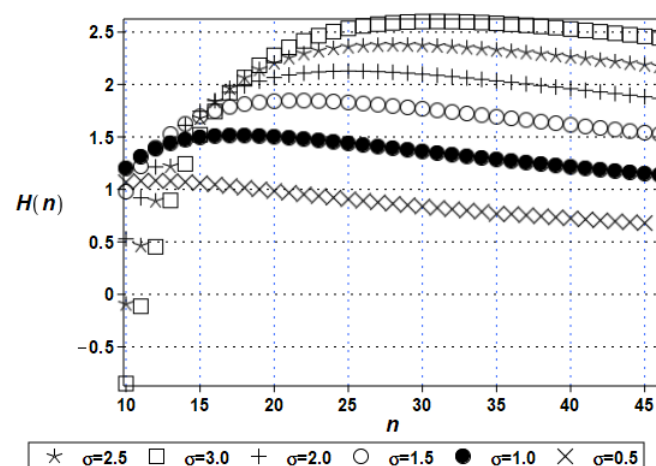


**Figure 4.** Convergence rate for the interval entropy computations.



Three different probability distributions having the same variability ranges have been tested to model statistical scattering of structural damping in this MEMS system, namely, in turn—Gaussian, uniform, and also the triangular one. The total number of random trials in the MCS algorithm has been set as 200,000 and probabilistic entropy has been computed in any second for a time period  $t \in [0.0, 50.0 \text{ s}]$ . The range of Gaussian distribution has been restricted following the three-sigma rule. The results of numerical simulation have been collected in Figures 5, 7, and 9 in the form of probabilistic Shannon entropies time variations, and also in the form of their logarithms, cf., Figures 6, 8, and 10; the right additional column has been added to better expose time fluctuations second by a second. These data have been contrasted for four different input coefficients of variation of structural damping  $\alpha(c) = [0.05, 0.10, 0.15, 0.20]$  to see an impact of the input statistical scattering of this damping.

Figures 5–10 show clearly that probabilistic entropies (and their logarithms) have the same patterns for all three different probability distributions and that they all reach extreme values at the very end of the simulated dynamic process. A comparison of Figure 3 (right) with Figures 5, 7, and 9 exhibits that the pattern of time fluctuations of the resulting CoVs and these adjacent to probabilistic entropies are almost the same. Generally, the variability ranges of all entropies for three different PDFs seem to be very similar to each other. However, as one could expect after the maximum entropy principle, the largest values of Shannon entropy are obtained when the damping coefficient has Gaussian distribution, then—in turn—for the uniform and triangular PDFs. It is also seen that the resulting probabilistic entropy is proportional to the input coefficient of variation of structural damping, i.e., they increase with each other.

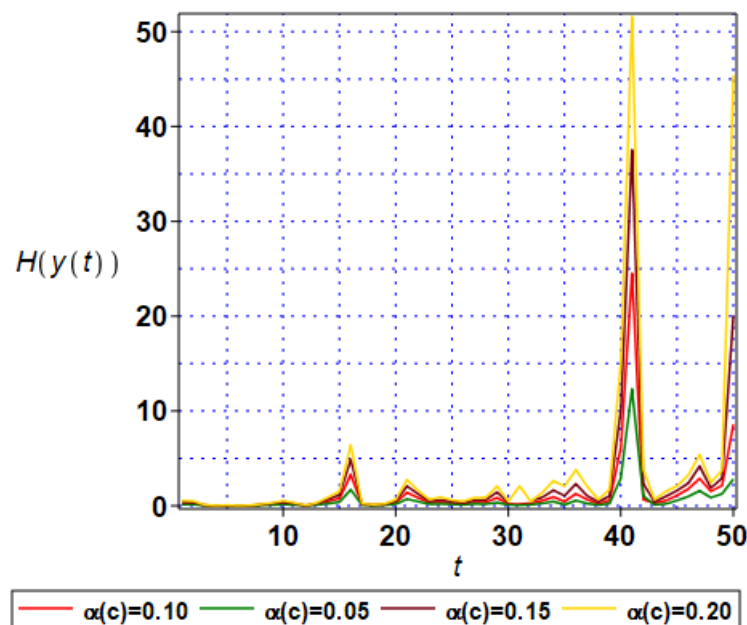


Figure 5. Shannon entropies time fluctuations for Gaussian structural damping.

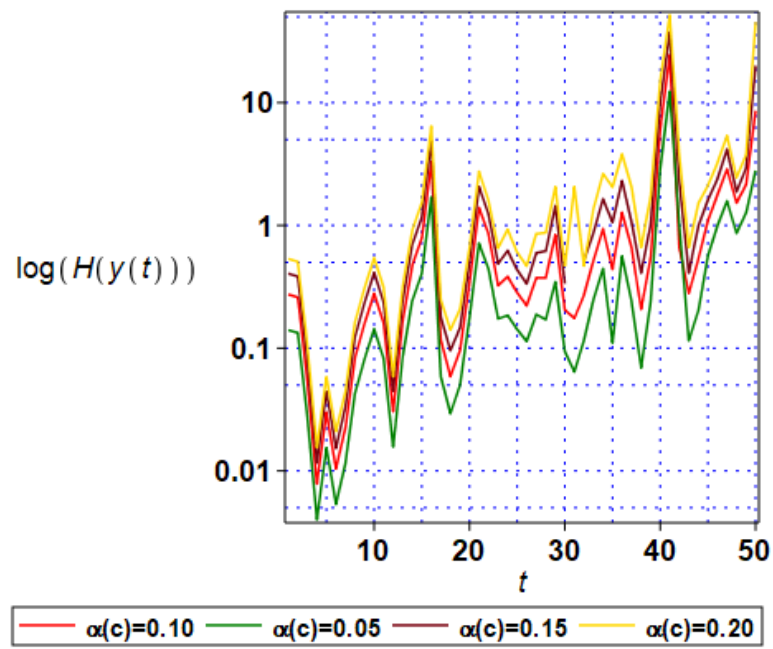


Figure 6. Shannon entropies logarithm time fluctuations for Gaussian structural damping.

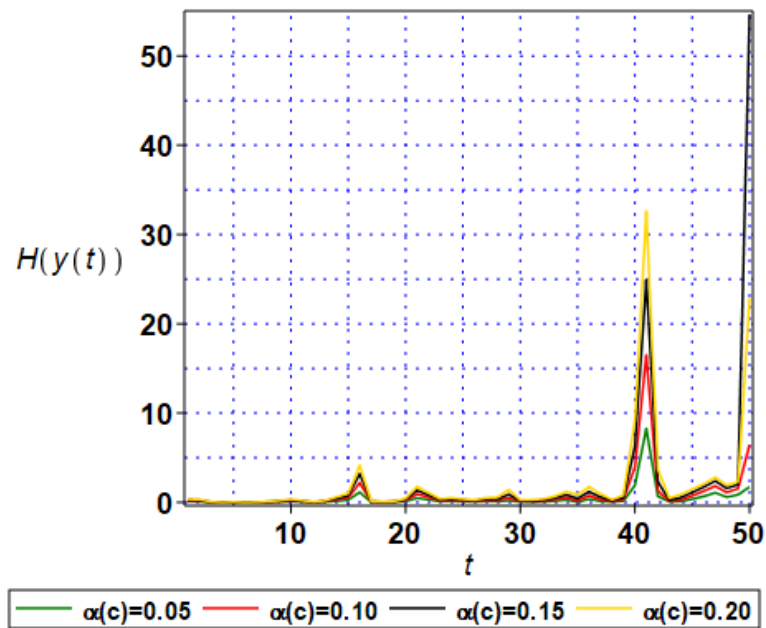


Figure 7. Shannon entropies time fluctuations for uniformly distributed structural damping.

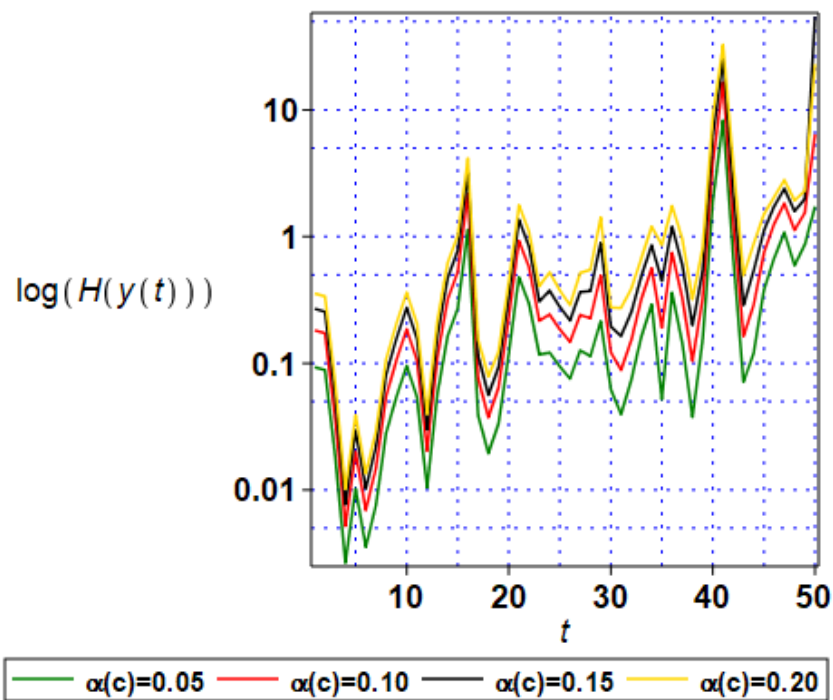


Figure 8. Shannon entropies logarithm time fluctuations for uniformly distributed structural damping.

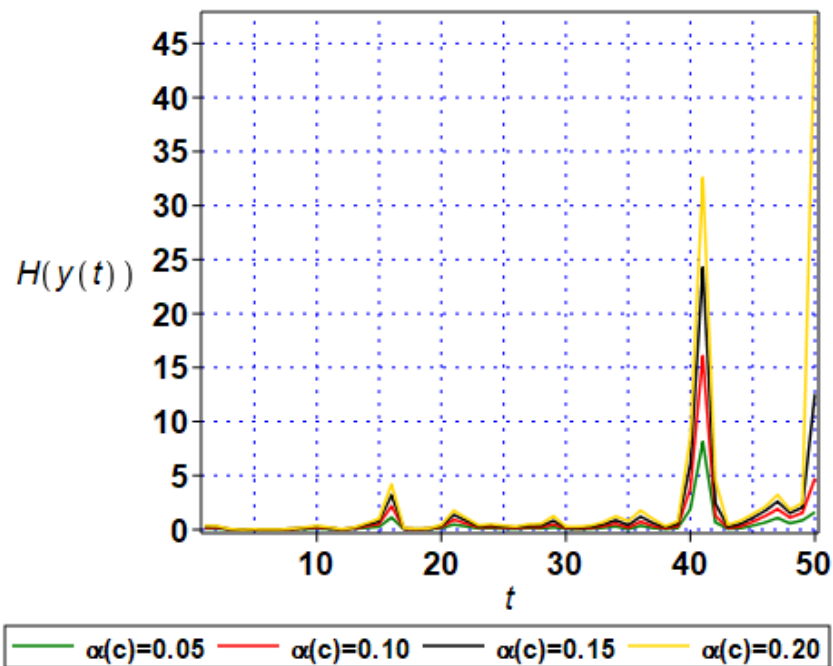
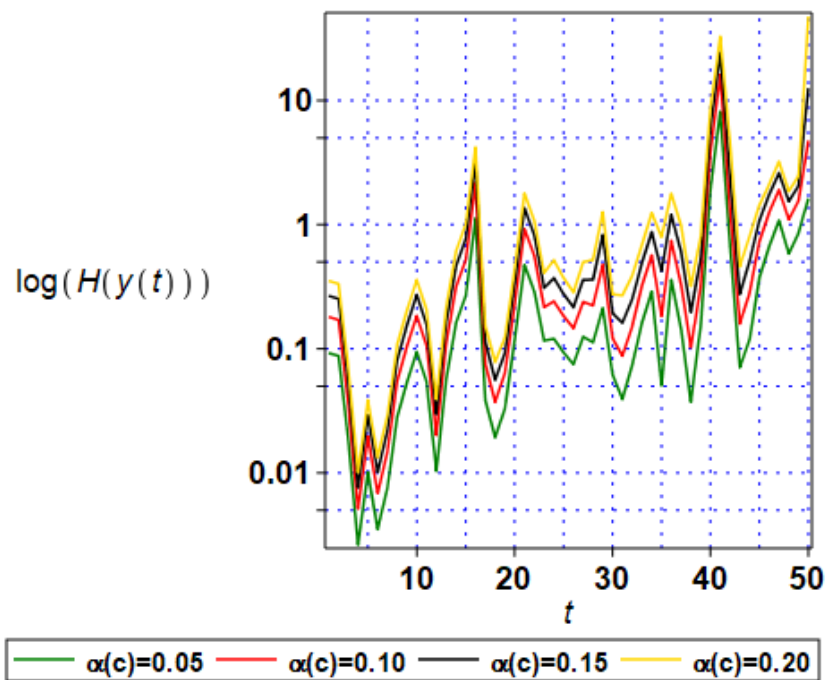


Figure 9. Shannon entropies time fluctuations for triangularly distributed structural damping.



**Figure 10.** Shannon entropies logarithm time fluctuations for triangularly distributed structural damping.

A very important aspect is that computational time relevant to determination probabilistic entropy is almost the same, while for the increasing number of random samples above 10%, it is even shorter than statistical estimation of the first two probabilistic moments of the structural response. If one could estimate the first four probabilistic characteristics (including also skewness and kurtosis [41]), then the entropy calculus brings definitely more information about uncertainty propagation with definitely smaller computer effort. This is seen for the single-degree-of-freedom system, whereas the Stochastic Finite Element Method analysis of large scale systems would show huge disproportion of computer power consumption. Therefore, a proper calculation and interpretation of probabilistic entropy may bring essential time savings while using the Monte Carlo simulation approach.

Although time variations of these entropies exhibit some remarkably high and rapid fluctuations, the mean values of probabilistic entropy increase systematically in each case study. It means that uncertainty (disorder) in each dynamical system subjected to harmonic excitation increases in the presence of random damping. This is, in turn, quite consistent with engineering practice and shows that this system becomes less and less predictable together with an increase of vibrations time. Finally, one may observe that this vibration undergoes some critical points, where the resulting CoV reaches huge extreme values, while the uncertainty level for the remaining part throughout this vibration process is a few times smaller. This especially happens while the mean value of the displacement is very close to the initial value (see Figure 4).

## 5. Concluding Remarks

A simulation-based approach for the determination of probabilistic entropy in some MEMS devices, whose dynamic response follows the Duffing equation, has been demonstrated in this work. A majority of the proposed approach has no upper bounds on the input uncertainty level and no limitation for the number of various design random parameters. Interval representation of the given probability density function applied together with the Monte Carlo simulation scheme of the structural response enables for re-

liable and relatively fast computation of probabilistic entropy propagation in many engineering systems including MEMS devices. As was demonstrated, it does not demand a large effort in the discretization of the resulting probability distribution—one can model non-Gaussian distribution of any physical, material, or geometrical parameters. It can be done both using some analytical solutions provided with the computer algebra programs like MAPLE as well as thanks to its common application with some commercial FEM systems (like COMSOL, ANSYS, or ABAQUS). It would be very instructive to compare the mechanical model presented and discussed above with a full multi-physics simulation of the electro-magneto-mechanical system vibrations to discover similarities and also possible divergence. An influence of the temperature field on the MEMS signal analysis and vibrations would be very important from the technological point of view [40], where uncertainty seems to be quite natural.

Probabilistic Shannon entropy exhibits almost the same extreme values and the corresponding time moments as the output coefficient of variation of the dynamical system response. It has been demonstrated that both approaches based on probabilistic characteristics of the structural responses and their probabilistic entropy exhibit huge values, many times larger than in traditional civil engineering structures, where such MEMS devices are applicable. Such a huge output uncertainty needs special modelling attention and excludes application of less precise stochastic methods like lower order expansions; in this context, the proposed entropy-based structural analysis has no limitations. That is why this methodology seems to be very promising in further uncertainty quantification in elasto-dynamics; civil engineering applications of this apparatus can be especially beneficial in seismic uncertainty analysis [42]. However, numerical Shannon entropy determination may be sensitive to the PDF partitioning of the structural response, so some initial sensitivity analysis would be required. Further computational experiments should include relative probabilistic entropies analysis, where an additional divergence (like Kullback–Leibler, for instance) in between a forced vibration and the resulting extreme structural response, would be considered. A possible alternative for the Monte Carlo simulation-based determination of entropy could be the Probability Transformation Method proposed by Falsone [43].

**Author Contributions:** Conceptualization, M.K. and A.C.; methodology, M.K.; software, A.C.; validation, M.K. and A.C.; formal analysis, M.K.; investigation, M.K. and A.C.; resources, A.C.; data curation, A.C.; writing—original draft preparation, M.K.; writing—review and editing, M.K. and A.C.; visualization, M.K.; supervision, A.C.; project administration, M.K.; funding acquisition, M.K.; literature overview, M.K. and A.C. All authors have read and agreed to the published version of the manuscript.

**Funding:** This paper was written in the framework of the research grant OPUS no 2021/41/B/ST8/02432, entitled “Probabilistic entropy in engineering computations”, and is sponsored by the National Science Center in Poland.

**Institutional Review Board Statement:** This does not apply in case of this manuscript.

**Informed Consent Statement:** This does not apply in case of this manuscript.

**Data Availability Statement:** This does not apply in case of this manuscript.

**Acknowledgments:** This does not apply in case of this manuscript.

**Conflicts of Interest:** Both authors declare no conflict of interest.

## References

1. Shannon, C.E. A mathematical theory of communication. *Part I Bell Sys. Tech. J.* **1948**, *27*, 379–423.
2. Shannon, C.E. A mathematical theory of communication. *Part II Bell Sys. Tech. J.* **1948**, *27*, 623–656.
3. Kamiński, M. On Shannon entropy computations in selected plasticity problems. *Int. J. Num. Meth. Engrg.* **2021**, *122*, 5128–5143.
4. Beirlant, J.; Dudewicz, E.J.; Gyoerfi, L.; van der Meulen, E.C. Nonparametric entropy estimation: An overview. *Int. J. Math. Stat. Sci.* **1997**, *6*, 17–39.

5. Renyi, A. On measures of entropy and information. In Proceedings of the Fourth Berkeley Symposium on Mathematical Statistics and Probability, Berkeley, CA, USA, 20 June–30 July 1960; pp. 547–561.
6. Renyi, A. On the dimension and entropy of probability distributions. *Acta Math. Acad. Sci. Hung.* **1959**, *10*, 193–215.
7. Abe, S.; Rajagopal, A.K. Revisiting disorder and Tsallis statistics. *Science* **2003**, *300*, 249–251.
8. Kamiński, M. Tsallis entropy in dual homogenization of random composites using the stochastic finite element method. *Int. J. Num. Meth. Engrg.* **2018**, *113*, 834–857.
9. Tsallis, C. *Introduction to Non-extensive Statistical Mechanics: Approaching a Complex World*; Springer: New York, NY, USA, 2009.
10. Tsallis, C. Possible generalization of Boltzmann-Gibbs statistics. *J. Stat. Phys.* **1988**, *52*, 479–487.
11. Cornfeld, I.P.; Fomin, S.F.; Sinai, Y.A. *Ergodic Theory*; Springer: Berlin/Heidelberg, Germany, 1981.
12. Latora, V.; Baranger, M. Kolmogorov-Sinai entropy rate versus physical entropy. *Phys. Rev. Letters* **1999**, *82*, 520–523.
13. Leydesdorff, L. The production of probabilistic entropy in structure/action contingency relations. *J. Soc. Evol. Syst.* **1995**, *18*, 339–356.
14. Li, H.S. Maximum entropy method for probabilistic bearing strength prediction of pin joints in composite laminates. *Compos. Struct.* **2013**, *106*, 626–634.
15. Shi, X.; Teixeira, A.P.; Zhang, J.; Soares, C.G. Structural reliability analysis based on probabilistic response modelling using the maximum entropy method. *Eng. Struct.* **2014**, *70*, 106–116.
16. Erickson, G.J.; Smith, C.R. *Maximum-Entropy and Bayesian Methods in Science and Engineering*; Kluwer: Dordrecht, The Netherlands; Boston, MA, USA; London, UK, 1988.
17. Kamiński, M. *The Stochastic Perturbation Method for Computational Mechanics*; Wiley: Chichester, UK, 2013.
18. Cruz, M.E.; Patera, A.T. A parallel Monte-Carlo finite element procedure for the analysis of multicomponent media. *Int. J. Num. Meth. Engrg.* **1995**, *38*, 1087–1121.
19. Hurtado, J.E.; Barbat, A.H. Monte-Carlo techniques in computational stochastic mechanics. *Arch. Comput. Meth. Engrg.* **1998**, *5*, 3–30.
20. Liu, Y.K. *Probabilistic Theory of Structural Dynamics*; McGraw-Hill: New York, NY, USA, 1967.
21. Liu, H.; Chen, W.; Sudjianto, A. Relative entropy based method for probabilistic sensitivity analysis in engineering design. *ASME J. Mech. Des.* **2006**, *128*, 326–336.
22. Kullback, S.; Leibler, R.A. On information and sufficiency. *Ann. Math. Statist.* **1951**, *22*, 79–86.
23. Hellinger, E. Neue begründung der theorie quadratischer formen von unendlichvielen veraenderlichen. *J. Für Die Reine Und Angew. Math.* **1909**, *136*, 210–271.
24. Chernoff, H. A measure of asymptotic efficiency for tests of a hypothesis based on the sum of observations. *Ann. Math. Stat.* **1952**, *23*, 493–507.
25. Mahalanobis, P. On the generalized distance in statistics. *Proc. Natl. Inst. Sci. India* **1936**, *2*, 49–55.
26. Bhattacharyya, A. On a measure of divergence between two statistical populations defined by their probability distributions. *Bull. Calcutta Math. Soc.* **1943**, *35*, 99–109.
27. Corigliano, A.; Ardito, R.; Comi, C.; Frangi, A.; Ghisi, A.; Mariani, S. *Mechanics of Microsystems*; John Wiley & Sons: Hoboken, NJ, USA, 2018. ISBN 978-1-119-05383-5.
28. Lucas, V.; Golinval, J.C.; Paquay, S.; Nguyen, V.D.; Noels, L.; Wu, L. A stochastic computational multiscale approach; Application to MEMS resonators. *Comput. Methods Appl. Mech. Eng.* **2015**, *294*, 141–167. <https://doi.org/10.1016/j.cma.2015.05.019>.
29. Sung, S.H.; Park, J.W.; Nagayama, T.; Jung, H.J.; A multi-scale sensing and diagnosis system combining accelerometers and gyroscopes for bridge health monitoring. *Smart Mat. Struct.* **2014**, *23*, 015005.
30. Batou, A.; Ritto, T.G.; Sampaio, R. Entropy propagation analysis in stochastic structural dynamics: Application to a beam with uncertain cross sectional area. *Comput. Mech.* **2014**, *54*, 591–601.
31. Wang, R.M.; Zhang, H.M.; Zhang, Y.N. Bifurcation and vibration resonance in the time delay Duffing system with fractional internal and external damping. *Meccanica* **2022**, *57*, 999–1015. <https://doi.org/10.1007/s11012-022-01483-y>.
32. Forsythe, G.E.; Malcolm, M.A.; Moler, C.B. *Computer Methods for Mathematical Computations*; Prentice Hall: Hoboken, NJ, USA, 1977.
33. Björck, A. *Numerical Methods for Least Squares Problems*; SIAM: Philadelphia, PA, USA, 1996.
34. Cover, T.M.; Thomas, J.A. *Elements of Information Theory*, 2nd ed.; Wiley-Interscience: New York, NY, USA, 2006.
35. Al-Omari, A.I. Estimation of entropy using random sampling. *J. Comput. Appl. Math.* **2014**, *261*, 95–102.
36. Xu, Z.; Shi, Y.; Zhao, Q.; Li, W.; Liu, K. Extreme interval entropy based on symbolic analysis and a self-adaptive method. *Entropy* **2019**, *21*, 238–256.
37. Shao, Y.; Hahn, M.G. Limit theorems for the logarithm of sample spacings. *Stat. Prob. Lett.* **1995**, *24*, 121–132.
38. Vasicek, O. A test for normality based on sample entropy. *J. Roy. Stat. Soc.* **1976**, *38*, 54–59.
39. Feller, W. *An Introduction to Probability Theory and Applications*; Wiley: New York, NY, USA, 1965.
40. Comi, C.; Zega, V.; Corigliano, A. Non-linear mechanics in resonant inertial micro sensors. *Int. J. Non-Linear Mech.* **2020**, *120*, 103386. <https://doi.org/10.1016/j.ijnonlinmec.2019.103386>.
41. Kamiński, M.; Corigliano, A. Numerical solution of the Duffing equation with random coefficients. *Meccanica* **2015**, *50*, 834–857.
42. Zembaty, Z. Non-stationary random vibrations of a shear beam under high frequency seismic effects. *Soil Dyn. Earthq. Engrg.* **2007**, *27*, 1000–1011.
43. Falsone, G.; Settineri, D. Explicit solutions for the response probability density function of nonlinear transformations of static random inputs. *Probabilistic Eng. Mech.* **2013**, *33*, 79–85.